2022 年臺灣國際科學展覽會
優勝作品專輯

作品編號 **030024**

參展科別 化學

作品名稱 **In Silico Modeling of Lovastatin Analogues as Inhibitors of HIV-1 Nef Protein**

得獎獎項

國　　家 **Philippines**

就讀學校 **Philippine Science High School - Main Campus**

指導教師 **Julius Victorius A. Saluria**

作者姓名 **Anne Maricar T. Maralit**

Ron Angelo A. Gelacio

Roxanne D. Bangsil

關鍵詞 **lovastatin、HIV-1 Nef-AP-1 complex、molecular docking**

作者照片


anne maricar marsit
Julius Victorius Saluria
roxanne bangsil
You

ABSTRACT

Currently, no method can completely eliminate the human immunodeficiency virus (HIV) in an infected person. HIV employs an accessory protein called Nef that forms a complex with cellular AP-1, preventing detection of HIV-infected cells. Lovastatin has been recently identified to inhibit the formation of said Nef-AP-1 complex, but its effective concentration is remarked to be far higher than other Nef inhibitors. This study aims to develop a modified lovastatin molecule exhibiting higher binding affinity to the HIV-1 Nef protein than lovastatin *in silico*. Modified lovastatin molecules based on the interaction map of lovastatin with Nef were modeled, and flexible ligand-flexible receptor docking to the Nef binding site was performed using AutoDock Vina. Residues within the Nef binding site identified by Liu et al. (2019) to be crucial (Glu-63, Val-66, Phe-68, Asp-108, Leu-112, Tyr-115) were set as flexible. Fragment-based drug design was utilized to append molecular fragments to lovastatin in order to maximize its interactions with said crucial residues. From the fragment-based approach, molecule F4 ((1S,3S)-8-{2-[(2R,4R)-4-chloro-6-oxooxan-2-yl]ethyl}-3-(hydroxymethyl)-7-methyl 1,2,3,4-tetrahydronaphthalen-1-yl 4-aminobenzoate) exhibited a binding affinity of -9.0 kcal/mole, and its estimated IC_{50} ranges between 0.25-0.51 μM which is at least 7.5 times lower than the reported IC_{50} of lovastatin from literature. This study presents insights on the key modifications to improve lovastatin as an HIV-1 Nef inhibitor and pertinent information about the Nef binding site for future drug development studies.

INTRODUCTION

Background of the Study

Currently, no method can completely eliminate the human immunodeficiency virus (HIV) in an infected person. Antiretroviral therapy does limit HIV by targeting cells harboring active viruses, but it cannot target latent HIV reservoirs (Cary & Peterlin, 2016), resulting in the persistence of HIV in an infected individual. One approach towards eliminating these HIV reservoirs is developing inhibitors of HIV-1 Nef. Nef is an accessory protein of HIV-1 that reduces the amount of major histocompatibility complex class I (MHC-I) molecules present on the surface of infected cells (Basmaciogullari & Pizzato, 2014). This prevents subsequent detection and elimination of infected cells by cytotoxic T lymphocytes (Collins et al., 1998).

Recently, lovastatin, a part of the statin class of drugs, has been identified as a potential Nef inhibitor. It has been shown to directly target and bind to Nef as well as inhibit the formation of the Nef-AP-1 complex, which is crucial for MHC-I downregulation (Liu et al., 2019). However, the IC_{50} of lovastatin has only been observed at around 3.788 μM, which was remarked to be far higher than other Nef inhibitors (Painter et al., 2020).

Objectives of the Study

This study aims to develop a modified lovastatin molecule that has a higher binding affinity to the HIV-1 Nef protein than lovastatin through *in silico methods* so that a more potent drug with therapeutic concentrations lower than that reported by Liu et al. (2019) and may achieve similar effects to lovastatin may be developed and used in clinical trials..

Lovastatin molecules with modified groups based on the previously identified interactions between lovastatin and key amino acid residues of the HIV-1 Nef binding site were modeled. The binding affinities of these analogues to Nef were determined using AutoDock Vina and compared to that of lovastatin and with other analogues.

Significance of the Study

Finding effective analogues of lovastatin that require lower concentrations to inhibit Nef may open up possibilities of conducting *in vivo* trials and clinical trials in the future. This may also lead to a better understanding of the interactions of Nef with lovastatin and its analogues. This could also inspire and pave the way for the further development of new compounds that may target HIV-1 Nef protein, and ultimately, the development of a drug that may eliminate HIV from an infected person's body.

Scope and Limitations

The study was done using MarvinSketch to model the lovastatin analogues, AutoDock Vina to run the protein-ligand docking of said analogues, and PyMol to visualize the top docking poses. The molecular databases that were used are PubChem for the lovastatin molecule and RCSB Protein Data Bank for the HIV-1 Nef protein. The identified analogues were not synthesized in the laboratory to determine the feasibility of doing so, nor were confirmatory tests done *in vitro* to validate the results from the docking calculations.

The study only examined analogues of lovastatin and did not examine analogues of other members of the statin class of drugs nor previously identified Nef inhibitors. The study also examined the effects of these analogues on the HIV-1 Nef protein only, and no other accessory proteins of HIV-1 were considered.

METHODOLOGY

Process Flowchart

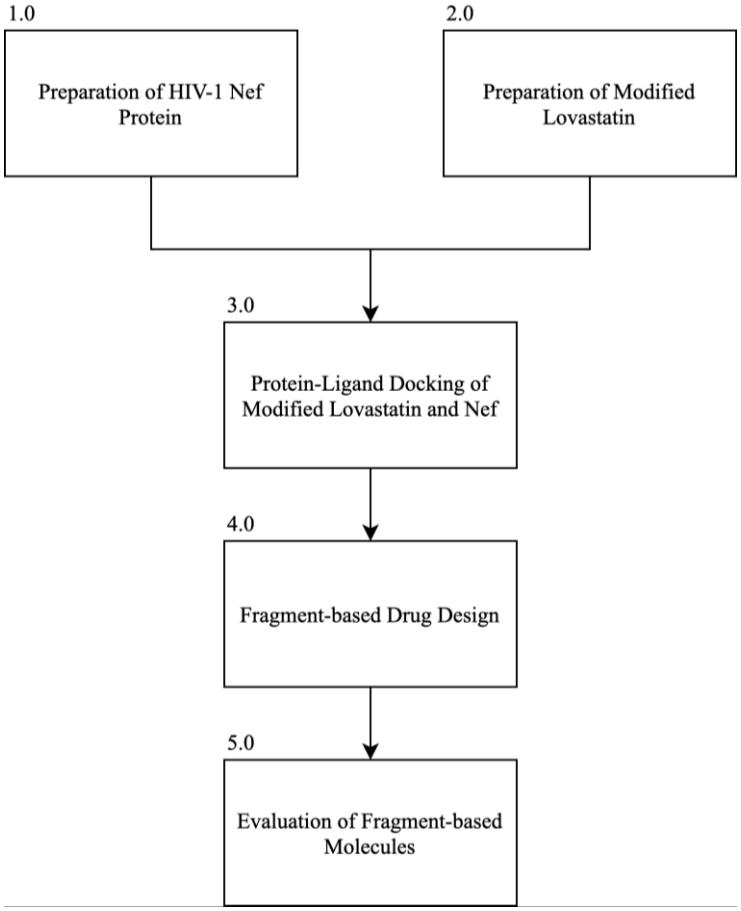

Preparation of HIV-1 Nef Protein

The crystal structure file of the HIV-1 Nef protein (in .pdb format) was downloaded from the RCSB Protein Data Bank (code: 4EMZ). The Nef protein was prepared using AutoDock Tools by removing the water molecules present in the structure, adding polar hydrogens, and adding Kollmann charges. The processed Nef protein file was exported (in .pdbqt format). The grid parameters of the previously identified docking site of HIV-1 Nef by Liu et al. (2019) were set using AutoDock Tools, and the corresponding grid dimension file (in .txt format) were exported.

Preparation of Modified Lovastatin

The 3D structure file of lovastatin (in .sdf format) was downloaded from the PubChem database. The lovastatin structure file was then converted to a .pdb format using MarvinSketch. The .pdb lovastatin file was prepared using AutoDock Tools by setting the number of rotatable bonds within the molecule, and the resulting .pdbqt file of the lovastatin file was exported.

The interaction map between lovastatin and the amino acid residues of the HIV-1 Nef docking site provided by Liu et al. (2019) was used as the basis in determining the modifications that were applied to lovastatin. The modification process was done in iterations wherein one region of the lovastatin molecule was modified by changing the functional groups present and gradually increasing said region's lipophilicity or hydrophilicity, before modifying other regions of the molecule.

The modified lovastatin molecules that were generated from this iterative process were drawn using MarvinSketch and exported as .pdb files. The .pdbqt structure files of these analogues were prepared in the same procedure outlined above for lovastatin.

Protein-Ligand Docking of Modified Lovastatin and Nef

AutoDock Vina was launched using Command Prompt. The HIV-1 Nef protein receptor file, the structure file of a modified lovastatin molecule, and a configuration file (consisting of the grid dimensions and other settings including the maximum energy range between the binding energies and exhaustiveness) were specified as inputs. The outputs consisting of a log file (in .txt format) and a .pdbqt output file of the docking poses of the selected analogue were also specified. After setting these specifications, the docking calculations were performed using AutoDock Vina. The entire process was repeated until all

analogues were docked. The same receptor file and configuration file was used throughout the docking process.

After performing the docking calculations on all lovastatin analogues, PyMol was used to visualize the docking poses of a lovastatin analogue to the HIV-1 Nef protein. The .pdbqt file of the Nef protein was imported into PyMol, followed by the .pdbqt output file of a selected lovastatin analogue. After importing, the docking poses of the lovastatin analogue and Nef were then visualized. The top binding pose that interacted with key residues within the Nef binding site, namely Glu-63 and Phe-68, was selected. The binding affinity of said top binding pose was also reported. This process was repeated with the .pdbqt output files of the rest of the individually modified lovastatin molecules.

Fragment-based Drug Design

A newly discovered binding pocket involving Val-66 within the Nef binding site was explored using fragment-based drug design. Using MarvinSketch, different molecular fragments were added to the lovastatin molecule in order to maximize the interactions between the new binding pocket and the previously mentioned key residues. The structure files of these fragment-based molecules were prepared using AutoDock Tools in the same manner as the individually modified lovastatin molecules. These were then docked using AutoDock Vina, and the generated results were analyzed using PyMol following the process outlined above.

Evaluation of Fragment-based Molecules

Lipinski's Rule of 5 was used as the basis to evaluate the fragment-based molecules and to identify the most viable drug candidate that will be compared against lovastatin. MarvinSketch was used to calculate the parameters specified by Lipinski et al. (1997) for the

fragment-based molecules, namely their molecular weight, partition coefficient, and the number of H-bond donors and acceptors. The molecules that meet the threshold values for these parameters were identified, and their inhibitory constants (K_i) and IC_{50} were then estimated.

RESULTS AND DISCUSSION

The effects of modifying individual regions of the lovastatin molecule were explored first. Figure 1 summarizes these modifications. The main modifications done to the molecule include extending the carbon chain of the ester group, replacing the hydroxyl group of the six-membered lactone, and aromatizing one of the fused rings of lovastatin.

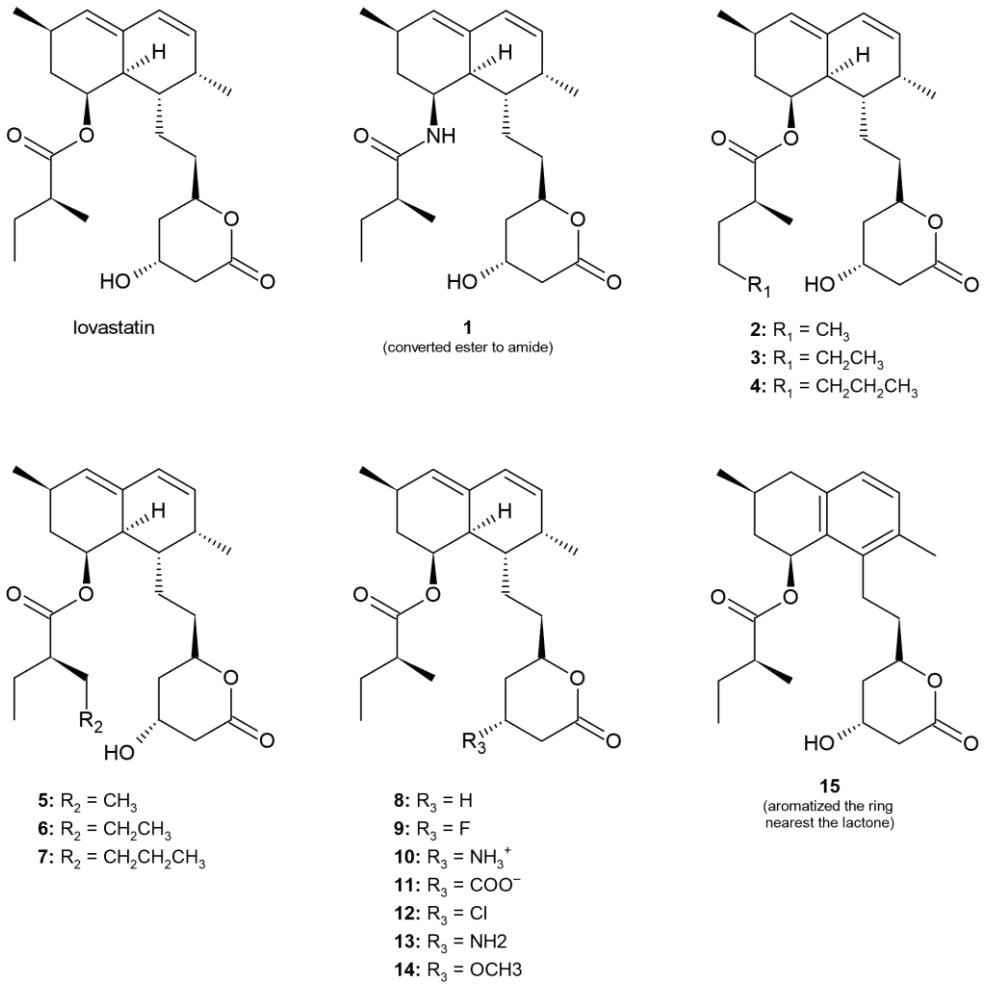

Figure 1. Structures of lovastatin and the modified lovastatin molecules.

After docking each molecule with AutoDock Vina, the pose with the highest binding affinity which exhibited interactions with Glu-63 or Phe-68 was reported. Liu et al. (2019) identified these residues within the Nef binding pocket to be crucial in inhibiting the formation of the Nef-AP-1 complex. The selected top binding affinity per molecule is shown in Table 1.

Table 1. Top Binding Affinities of Lovastatin Molecules Interacting with Glu-63 and Phe-68 of Nef

Ligand	Top Binding Affinity (kcal/mol)
lovastatin	-7.9
1	-8.1
2	-8.3
3	-8.1
4	-8.0
5	-8.2
6	-7.9
7	-8.2
8	-7.8
9	-8.1
10	-8.5
11	-7.8
12	-8.1
13	-8.4
14	-7.8
15	-8.4

The top docking pose of lovastatin can be seen in Figure 2. This is very similar to the docking pose of lovastatin presented by Liu et al. (2019), where the hydroxyl group of the lactone exhibits hydrogen-bonding (H-bonding) interactions with Glu-63 and the fused ring system interacts with Phe-68.

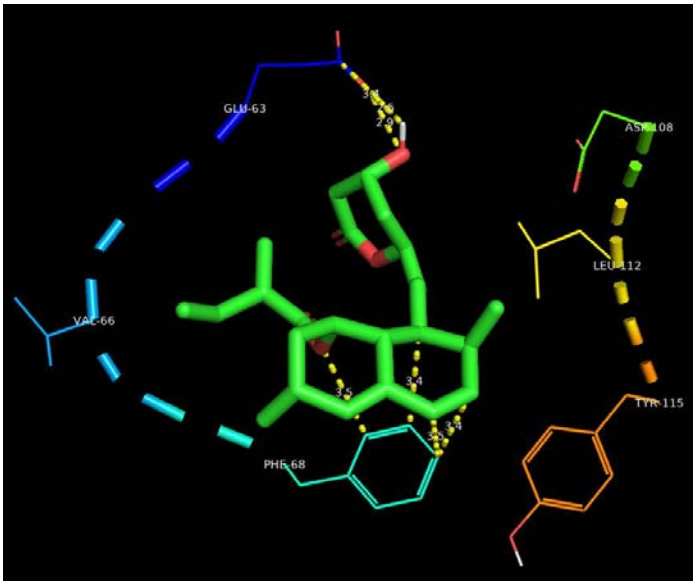

Figure 2. The top docking pose of lovastatin interacting with Glu-63 and Phe-68. Yellow dashes indicate interactions between the molecule and nearby amino acid residues.

Modifying the ester group

Molecules **1** to **7** involved the modification of the ester group present in lovastatin. This ester group was identified by Liu et al. (2019) to exhibit some hydrophobic interactions with Leu-112 in the Nef binding pocket, so the appropriate modifications for this ester group would be to extend its carbon chain. The top docking pose of molecules **1** to **7** as visualized in PyMol can be seen in Figure 3.

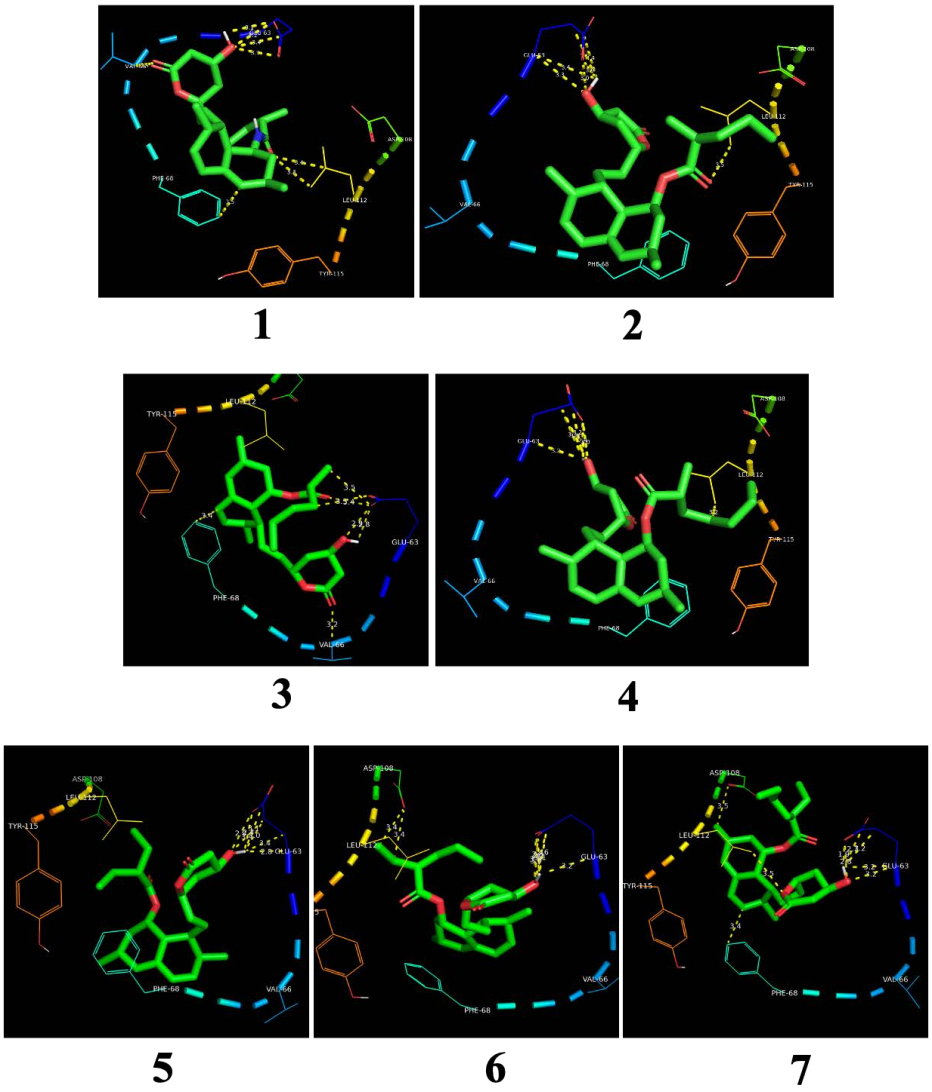

Figure 3. The top docking pose of molecules **1** to **7** interacting with Glu-63 and Phe-68. Yellow dashes indicate interactions between the molecule and nearby amino acid residues.

Molecule **1** where the ester is replaced by an amide showed a slight increase in the binding affinity to about −8.1 kcal/mol. Molecules **2** and **5** which feature an additional methyl (-CH_3) group in the ethyl and methyl group of the ester, respectively, have higher binding affinities than lovastatin at −8.3 kcal/mol (**2**) and −8.2 kcal/mol (**5**). The increase in binding affinities observed in these molecules can be attributed to the increase in London dispersion forces (LDF) between the molecule and the side chains of the Nef binding site residues,

particularly near the Leu-112 residue as seen in Figure 3, due to the addition of the methyl group.

Molecules **3** and **4** featured the extension of the ester's ethyl group by two and three more carbons, respectively. However, these molecules exhibited lower binding affinities than **2** at −8.1 kcal/mol (**3**) and −8.0 kcal/mol (**4**). This decrease in binding affinities can be explained by the nature of the longer carbon chain of the ester. Due to the bulkier carbon chain, optimal conformations within the binding pocket that maximize the interactions of the molecule with key residues in Nef may be discouraged from forming. Therefore, this effect may lower their binding affinities despite the theoretically higher LDFs associated with longer carbon chains. This trend of decreasing binding affinities as more carbons are added to the ester group can also be seen in molecules **6** and **7**, which both exhibit lower binding affinities per additional carbon than molecule **5** as seen in Table 1.

Replacing the hydroxyl group of the lactone

Molecules **8** to **14** involved the modification of the hydroxyl (-OH) substituent within the lactone group of lovastatin. Liu et al. (2019) identified the hydroxyl group to be an H-bond donor to Glu-63 in the Nef binding pocket, so the main modifications involved increasing or decreasing the H-bond donor capacity of the lactone substituent to explore its effects on the binding affinity of the molecule. The top docking pose of molecules **8** to **14** can be seen in Figure 4.

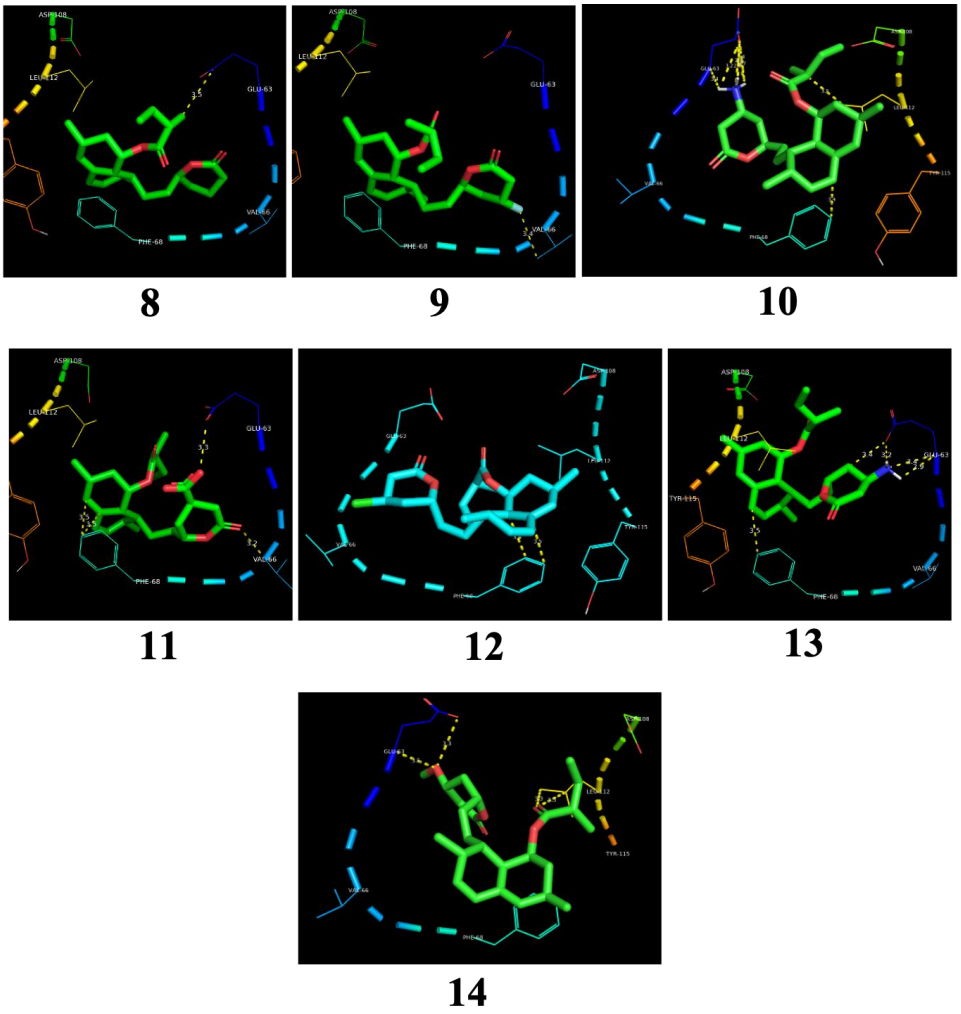

Figure 4. The top docking pose of molecules **8** to **14** interacting with Glu-63 and Phe-68. Yellow dashes indicate interactions between the molecule and nearby amino acid residues.

Molecule **8** wherein the hydroxyl group of the lactone is replaced by an H atom exhibited a lower binding affinity at −7.8 kcal/mol as seen in Table 1. This can be attributed to the fact that the hydroxyl group acts as an H-bond donor to Glu-63. Replacing the hydroxyl group with H removes this potential interaction as seen in the lack of a yellow dash towards Glu-63 in Figure 4. This leads to a lower binding affinity and also confirms the H-bond donor capability of the hydroxyl group suggested by Liu et al. (2019). Similarly, molecule **14** which replaces the hydroxyl group of the lactone with a methoxy group (-OCH_3) exhibited a lower binding affinity at −7.8 kcal/mol which may be caused by the decreased H-

bond donor capacity of the methoxy group. As seen in Figure 4, Glu-63 interacts directly with the O of the methoxy group instead.

Molecules **10** and **13** which replace the hydroxyl group of the lactone with an ammonium group ($-NH_3^+$) and an amino group ($-NH_2$), respectively, have higher binding affinities at −8.5 kcal/mol (**10**) and −8.4 kcal/mol (**13**). This increase can both be attributed to the increased H-bond donor capacity of the amino substituents which have more H atoms than the hydroxyl group. The favorable electrostatic interactions between the ammonium group of **10** and the negatively charged side chain of Glu-63 (which is deprotonated at physiological pH) may also explain its slightly higher binding affinity than **13**, whose amino substituent lacks a positive charge and consequently, favorable electrostatic interactions.

Molecule **11** which replaces the hydroxyl group of the lactone with a carboxylate group ($-COO^-$) showed a lower binding affinity at −7.8 kcal/mol. This slight decrease in binding affinity may be attributed to the repulsive interactions between $-COO^-$ and the negatively charged side chain of Glu-63 as mentioned before.

Molecules **9** and **12** feature the substitution of the hydroxyl group with the halogens F and Cl, respectively. Molecules **9** and **12** both exhibited a slight increase in binding affinity at −8.1 kcal/mol for both molecules. However, as seen in Figure 4, the conformation of molecule **12** compared to the original lovastatin molecule in Figure 2 is different with regards to the orientation of its lactone moiety. The lactone of **12** is now seen to be positioned near the Val-66 residue, with the Cl atom pointed towards it. This implies that the pocket where Glu-63 resides may be small and cannot accommodate bulky atoms and groups such as the Cl of **12** but can accommodate smaller groups like the F of **9** or the hydroxyl group of base lovastatin.

Aromatizing one of the fused rings

Liu et al. (2019) also identified that the Phe-68 residue, which features an aromatic side chain, interacts with the fused ring system of lovastatin. Thus, the effects of the aromatization of one of the two fused rings were also investigated. The top docking pose of molecule **15** can be seen in Figure 5.

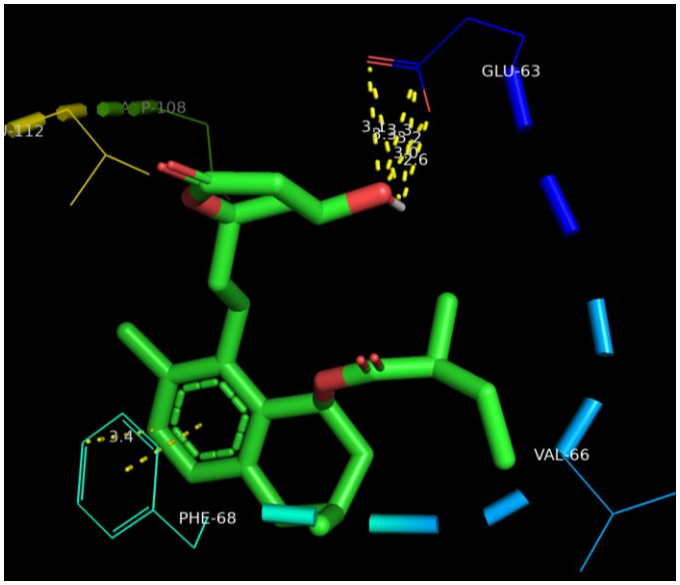

Figure 5. The top docking pose of molecule **15** interacting with Glu-63 and Phe-68. Yellow dashes indicate interactions between the molecule and nearby amino acid residues.

Molecule **15** features an aromatic ring in the bicyclic system nearer to the lactone, and it exhibited a higher binding affinity than the base lovastatin molecule at −8.4 kcal/mol as seen in Table 1. This increase in binding affinity may be attributed to favorable pi-stacking interactions which are described to be attractive, noncovalent interactions between aromatic systems (Egli, 2009). The presence of the aromatic ring allows **15** to exhibit pi-stacking interactions with the aromatic ring of Phe-68. This is supported by Figure 5 where the aforementioned interactions may be seen.

Among the 15 individually modified molecules, the only molecules that exhibited an increase in binding affinity by 0.5 kcal/mol or better are molecules **10**, **13**, and **15**. The two

main modifications present in these molecules, namely the increase in the H-bond donor capacity of the lactone substituent and the aromatization of one of the fused rings, are mainly aimed to maximize the interactions of the molecule with key residues Glu-63 and Phe-68. As seen in Table 1, the significant increase in binding affinity for these molecules compared to the rest suggest that these two main modifications are viable to include in the succeeding molecules.

Fragment-based drug design

As seen in Figure 4, the lactone moiety of molecule **12** is directed towards Val-66, which suggests the possibility of a new binding pocket. This potential binding pocket within the Nef protein was exploited using fragment-based drug design, a procedure where molecular fragments that exhibit interactions with certain pockets and residues within the protein may be appended (Murray & Rees, 2009). This approach was used to add new groups to **12** that will interact with Glu-63 while retaining the interaction of the lactone with Val-66 in the new pocket. The structures of these derivatives of **12** are shown in Figure 6.

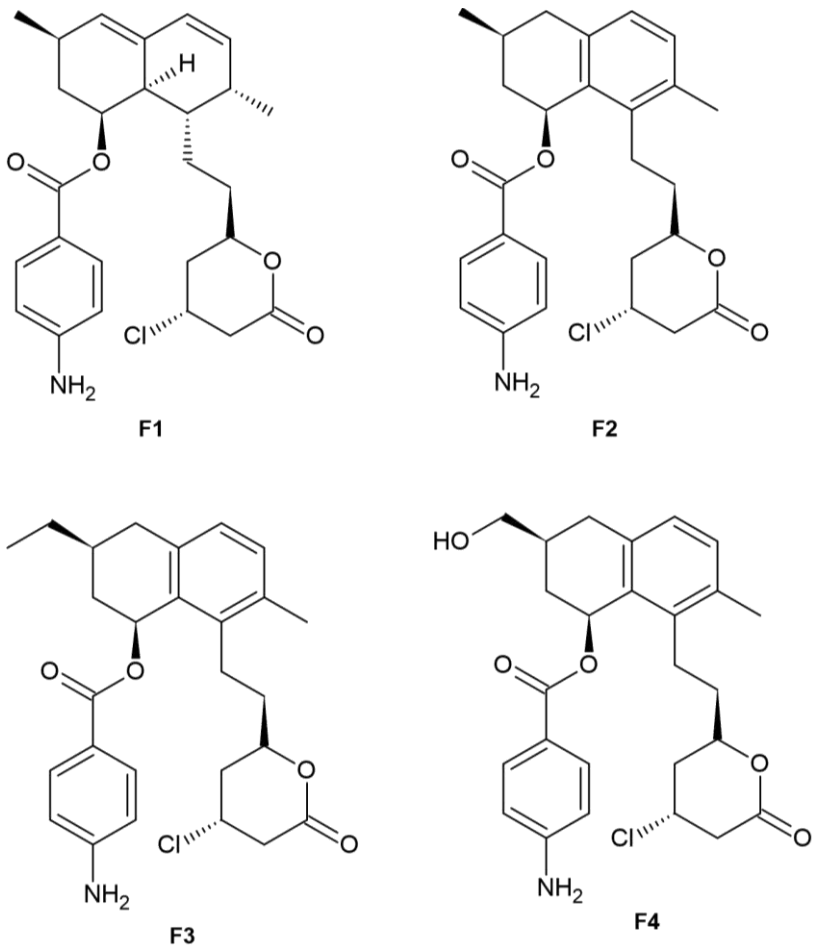

Figure 6. Structures of molecule **12** derivatives from fragment-based drug design.

These molecules were also docked using AutoDock Vina, and their top binding affinity which exhibited interactions with Glu-63, Phe-68, and Val-66 is recorded in Table 2. The docking poses of the top binding affinity of these molecules were also visualized using PyMol and are shown in Figure 7.

Table 2. Top Binding Affinities of Fragment-Based Lovastatin Molecules Interacting with Glu-63, Phe-68, and Val-66 of Nef

Ligand	Top Binding Affinity (kcal/mol)
F1	-8.5
F2	-9.0
F3	-8.9
F4	-9.0

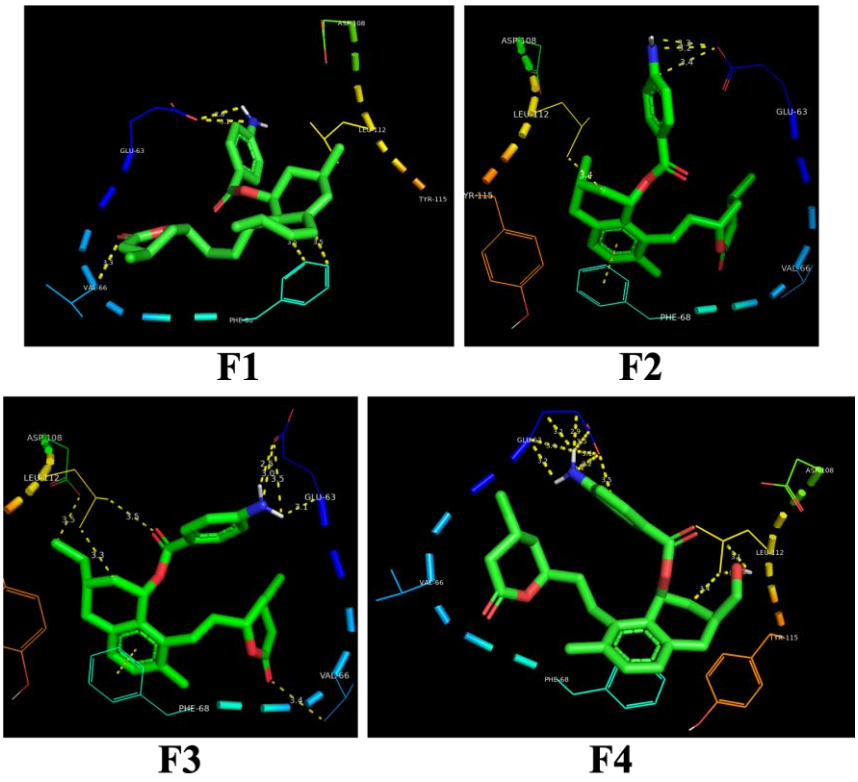

Figure 7. The top docking pose of molecules **F1** to **F4** interacting with Glu-63, Phe-68, and Val-66. Yellow dashes indicate interactions between the molecule and nearby amino acid residues.

As seen in Figure 6, the ester moiety of molecule **12** was modified and extended to interact with Glu-63. To prevent further complications in docking the new molecules, such as a decrease in docking accuracy associated with an increase in the number of rotatable bonds within a molecule (Erickson et al., 2003), a group with non-rotatable bonds such as a phenyl group with an amino substituent was selected to achieve the desired interactions with Glu-63.

Hence, molecule **F1** was modeled by replacing the 2-methylbutanoyl group of **12** with a para-aminobenzoyl (PAB) group. As seen in Table 2, **F1** exhibited an increase in binding affinity as compared to **12** at −8.5 kcal/mol which can be attributed to the additional H-bonding interactions between the PAB group and Glu-63 as shown in Figure 7.

To further increase the interactions of the molecule with Nef, **F1** was then modified by aromatizing one of the fused rings as shown in Figure 6 to generate molecule **F2**. Table 2 shows that there is a significant increase in the binding affinity of **F2** compared to **F1** at −9.0 kcal/mol, which may be attributed to additional pi-stacking interactions between the aromatized fused-ring system of **F2** and Phe-68 as seen in Figure 7.

One notable observation from the top pose of **F2** is that it also exhibited van der Waals interactions between one of the methyl substituents on the fused ring and Leu-112. Thus, possible interactions with Leu-112 were also explored. Molecule **F3** was derived from molecule **F2** by adding a methyl group to the aforementioned methyl substituent to determine if it would increase its hydrophobic interactions with Leu-112. However, **F3** exhibited a binding affinity of −8.9 kcal/mol which was slightly less than that of **F2**. Furthermore, as seen in Figure 7, the additional methyl group interacted with Asp-108 instead while Leu-112 interacted with the fused ring system and the new ester group.

With these findings, molecule **F4** was modeled by replacing the methyl group of **F3** with a hydroxyl group to explore possible interactions with Asp-108. The binding affinity of **F4** is comparable to that of **F2** at −9.0 kcal/mol (Table 2). However, as seen in Figure 7, the hydroxyl group interacted with Leu-112 instead of Asp-108.

Lipinski's Rule of Five

To determine the viability of the fragment-based molecules as drug candidates, **F2**, **F3**, and **F4** were subjected to analysis using Lipinski's Rule of 5. Lipinski's Rule of 5 predicts

that poor absorption or permeation of a drug is more likely to happen when its molecular weight exceeds 500 Da, its structure has more than five hydrogen bond donor sites or more than ten hydrogen bond acceptor sites, or it has a partition coefficient (log P) value greater than 5.0 (Lipinski et al., 1997). MarvinSketch was used to calculate the molecular weight, partition coefficient, and number of H-bond donors and acceptors of **F2**, **F3**, and **F4**, and the calculated data are recorded in Table 3.

Table 3. Summary of Lipinski's Rule of 5 data of **F2**, **F3**, and **F4**. Values violating the Rule of 5 are highlighted in red.

Ligand	Molecular Weight (g/mol)	Partition Coefficient (Log P)	H-bond Donor Sites	H-bond Acceptor Sites
F2	455.98	5.86	2	5
F3	470.01	6.26	2	5
F4	471.98	4.49	3	7

As seen in Table 3, only **F4** did not violate any of the conditions of Lipinski's Rule of 5, since **F2** and **F3** both exceeded the upper limit for the partition coefficient. Based on the data in Table 3, adding any more fragments to **F4** will most likely violate at least one condition of Lipinski's Rule of 5. Thus, the molecule **F4** was determined to be the most viable molecule from the study so far to compare against lovastatin.

Estimated IC_{50} of molecule F4

Liu et al. (2019) observed that the IC_{50} of lovastatin is around 3.788 μM, which was remarked to be far higher than other existing Nef inhibitors (Painter et al., 2020). To determine whether the estimated IC_{50} of **F4** is lower than that of lovastatin, its inhibitory constant, K_i, must be estimated first. Equation (1) gives the formula to calculate the corresponding K_i of a molecule from its binding affinity, ΔG (Dallakyan, 2010).

$$K_i = e^{\frac{\Delta G \times 4184}{RT}} \quad (1)$$

In Equation (1), ΔG is the binding affinity of the molecule calculated from docking (in kcal/mol), R is the gas constant (8.314 J/mol·K), and T is the temperature (298.15 K). Using the binding affinity of **F4** from Table 2, its K_i can be estimated at around 2.5×10^{-7}.

The IC_{50} of **F4** can then be estimated from the computed K_i value. According to Haupt et al. (2015), the corresponding IC_{50} of a drug can range from $IC_{50} = K_i$ to $IC_{50} = 2K_i$. Following this, the estimated range of possible IC_{50} values for **F4** is 0.25-0.51 μM, which is at least 7.5 times lower than the IC_{50} reported by Liu et al. (2019).

SUMMARY & CONCLUSION

Molecules **10**, **13**, and **15** exhibited higher binding affinities to HIV-1 Nef than lovastatin. The main modifications in these molecules, namely increasing the H-bond donor capacity of the lactone moiety and aromatizing one of the fused rings, maximized the interactions with key residues Glu-63 and Phe-68. Val-66 was also found to be a new potential binding pocket, and molecule **F4** was found to be the most viable drug candidate exhibiting the highest binding affinity to Glu-63, Val-66, Phe-68, and Leu-112 at −9.0 kcal/mol.

Overall, this study presents possible key modifications to improve lovastatin as an HIV-1 Nef inhibitor, a new potential lovastatin derivative (**F4**), and useful information about the key residues within the identified Nef binding pocket.

The properties of **F4** can be further analyzed through other in silico studies like quantitative structure-activity relationship (QSAR) analysis, as well as in vitro studies to determine its likely behavior within a cell-like environment. Moreover, the new binding pocket within the Nef binding site can be explored by other Nef inhibitors and may be used in further drug development studies against HIV-1 Nef.

REFERENCES

Basmaciogullari, S. P., & Pizzato, M. (2014). The activity of Nef on HIV-1 infectivity. *Frontiers in Microbiology*, *5*. https://doi.org/10.3389/fmicb.2014.00232

Cary, D. C., & Peterlin, B. M. (2016). Targeting the latent reservoir to achieve functional HIV cure. *F1000Research*, *5*, 1009. https://doi.org/10.12688/f1000research.8109.1

Collins, K. L., Chen, B. K., Kalams, S. A., Walker, B. D., & Baltimore, D. (1998). HIV-1 Nef protein protects infected primary cells against killing by cytotoxic T lymphocytes. *Nature*, *391*(6665), 397–401. https://doi.org/10.1038/34929

Dahabieh, M. S., Battivelli, E., & Verdin, E. (2015). Understanding HIV latency: The road to an HIV cure. *Annual Review of Medicine*, *66*(1), 407–421. https://doi.org/10.1146/annurev-med-092112-152941

Dallakyan, S. (2010, August 25). *How Autodock 4 converts binding energy (kcal/mol) into K_i.* AutoDock. http://autodock.scripps.edu/faqs-help/faq/how-autodock-4-converts-binding-energy-kcal-mol-into-ki.

Dekaban, G. A., & Dikeakos, J. D. (2017). HIV-I Nef inhibitors: a novel class of HIV-specific immune adjuvants in support of a cure. *AIDS Research and Therapy*, *14*(1). https://doi.org/10.1186/s12981-017-0175-6

Egli, M. (2009). On stacking. *Structure and Function*, 177–196. https://doi.org/10.1007/978-90-481-2888-4_7

Erickson, J. A., Jalaie, M., Robertson, D. H., Lewis, R. A., & Vieth, M. (2003). Lessons in molecular recognition: The effects of ligand and protein flexibility on molecular docking accuracy. *Journal of Medicinal Chemistry, 47*(1), 45–55. https://doi.org/10.1021/jm030209y

Foster, J. L., & Garcia, J. V. (2008). HIV-1 Nef: at the crossroads. *Retrovirology*, *5*(1), 84. https://doi.org/10.1186/1742-4690-5-84

Haupt, L. J., Kazmi, F., Ogilvie, B. W., Buckley, D. B., Smith, B. D., Leatherman, S., Paris, B., Parkinson, O., & Parkinson, A. (2015). The reliability of estimating K_i values for direct, reversible inhibition of cytochrome P450 enzymes from corresponding IC_{50} values: A retrospective analysis of 343 experiments. *Drug Metabolism and Disposition, 43*(11), 1744–1750. https://doi.org/10.1124/dmd.115.066597

Huey, R., Morris, G. M., & Forli, S. (2012). *Using AutoDock 4 and AutoDock Vina with AutoDockTools: A tutorial* [PDF]. The Scripps Research Institute. http://autodock.scripps.edu/faqs-help/tutorial/using-autodock-4-with-autodocktools/2012_ADTtut.pdf

Khan, S. U., Ahemad, N., Chuah, L.-H., Naidu, R., & Htar, T. T. (2020). Illustrated step by step protocol to perform molecular docking: Human estrogen receptor complex with 4-hydroxytamoxifen as a case study. *Progress in Drug Discovery & Biomedical Science*, *3*(1). https://doi.org/10.36877/pddbs.a0000054.

Lipinski, C., Lombardo, F., Dominy, B., & Feeney, P. (1997). Experimental and computational approaches to estimate solubility and permeability in drug discovery and development settings. *Advanced Drug Delivery Reviews, 23*(1-3), 3–25. doi:10.1016/s0169-409x(96)00423-1

Liu, B., Zhang, X., Zhang, W., Wu, L., Jing, S., Liu, W., … Li, L. (2019). Lovastatin inhibits HIV-1-induced MHC-I downregulation by targeting Nef–AP-1 complex formation: A new strategy to boost immune eradication of HIV-1 infected cells. *Frontiers in Immunology*, *10*. https://doi.org/10.3389/fimmu.2019.02151

Murray, C. W., & Rees, D. C. (2009). The rise of fragment-based drug discovery. *Nature Chemistry, 1*(3), 187–192. https://doi.org/10.1038/nchem.217

Painter, M. M., Zimmerman, G. E., Merlino, M. S., Robertson, A. W., Terry, V. H., Ren, X., … Collins, K. L. (2020). Concanamycin A counteracts HIV-1 Nef to enhance immune clearance of infected primary cells by cytotoxic T lymphocytes. *Proceedings of the National Academy of Sciences*, *117*(38), 23835–23846. https://doi.org/10.1073/pnas.2008615117

Trott, O., & Olson, A. (2009). AutoDock Vina: Improving the speed and accuracy of docking with a new scoring function, efficient optimization, and multithreading. *Journal of Computational Chemistry, 31*, 455–461. https://doi.org/10.1002/jcc.21334

【評語】030024

It is very nice to use computer modeling to help the drug development. It is very thorough to check so many molecular structures. Fully utilize the advantage of computer modeling.

Some suggestions are listed below.

1. Keep page number on both report and presentation slides.
2. The fragment-based drug design has big structure difference from compound 1 to15. It needs more explanation the design concept and the reason to choose chloride substitute instead of a stronger binding amine group.
3. Since compounds have amine substituents in general has higher finding affinity, how about trying dual amine substitutes.